TOXICOLOGICAL SCIENCES **82**, 279–296 (2004)
doi:10.1093/toxsci/kfh223
Advance Access publication July 14, 2004

Human Respiratory Tract Cancer Risks of Inhaled Formaldehyde: Dose-Response Predictions Derived From Biologically-Motivated Computational Modeling of a Combined Rodent and Human Dataset

Rory B. Conolly,[1] Julia S. Kimbell, Derek Janszen,[3] Paul M. Schlosser, Darin Kalisak, Julian Preston,[2] and Frederick J. Miller

Center for Computational Systems Biology & Human Health Assessment, CIIT Centers for Health Research, Research Triangle Park, North Carolina 27709

Received April 27, 2004; accepted July 7, 2004

Formaldehyde inhalation at 6 ppm and above causes nasal squamous cell carcinoma (SCC) in F344 rats. The quantitative implications of the rat tumors for human cancer risk are of interest, since epidemiological studies have provided only equivocal evidence that formaldehyde is a human carcinogen. Conolly *et al.* (*Toxicol. Sci.* 75, 432–447, 2003) analyzed the rat tumor dose-response assuming that both DNA-reactive and cytotoxic effects of formaldehyde contribute to SCC development. The key elements of their approach were: (1) use of a three-dimensional computer reconstruction of the rat nasal passages and computational fluid dynamics (CFD) modeling to predict regional dosimetry of formaldehyde; (2) association of the flux of formaldehyde into the nasal mucosa, as predicted by the CFD model, with formation of DNA–protein cross-links (DPX) and with cytolethality/regenerative cellular proliferation (CRCP); and (3) use of a two-stage clonal growth model to link DPX and CRCP with tumor formation. With this structure, the prediction of the tumor dose response was extremely sensitive to cell kinetics. The raw dose-response data for CRCP are J-shaped, and use of these data led to a predicted J-shaped dose response for tumors, notwithstanding a concurrent low-dose-linear, directly mutagenic effect of formaldehyde mediated by DPX. In the present work the modeling approach used by Conolly *et al.* (ibid.) was extended to humans. Regional dosimetry predictions for the entire respiratory tract were obtained by merging a three-dimensional CFD model for the human nose with a one-dimensional typical path model for the lower respiratory tract. In other respects, the human model was structurally identical to the rat model. The predicted human dose response for DPX was obtained by scale-up of a computational model for DPX calibrated against rat and rhesus monkey data. The rat dose response for CRCP was used "as is" for the human model, since no preferable alternative was identified. Three sets of baseline parameter values for the human clonal growth model were obtained through separate calibrations against respiratory tract cancer incidence data for nonsmokers, smokers, and a mixed population of nonsmokers and smokers, respectively. Additional risks of respiratory tract cancer were predicted to be negative up to about one ppm for all three cases when the raw CRCP data from the rat were used. When a hockey-stick-shaped model was fit to the rat CRCP data and used in place of the raw data, positive maximum likelihood estimates (MLE) of additional risk were obtained. These MLE estimates were lower, for some comparisons by as much as 1,000-fold, than MLE estimates from previous cancer dose-response assessments for formaldehyde. Breathing rate variations associated with different physical activity levels did not make large changes in predicted additional risks. In summary, this analysis of the human implications of the rat SCC data indicates that (1) cancer risks associated with inhaled formaldehyde are *de minimis* (10^{-6} or less) at relevant human exposure levels, and (2) protection from the noncancer effects of formaldehyde should be sufficient to protect from its potential carcinogenic effects.

Key Words: **formaldehyde; human cancer risk; dosimetry; dose-response; clonal growth; DNA-protein cross-links; regenerative cellular proliferation; computational modeling; risk assessment.**

F344 rats that inhaled formaldehyde chronically at 6, 10, or 15 ppm (6 hr/day, 5 days/wk) developed nasal squamous cell carcinoma (SCC; Kerns *et al.*, 1983; Monticello *et al.*, 1996). These rodent tumors raised concern for the potential human carcinogenicity of formaldehyde, since human exposure to formaldehyde is widespread, although more typically in the range of a few parts per billion (Health Canada, 2001). Conolly *et al.* (2003) developed a biologically motivated computational model to describe the F344 rat SCC data and to predict dose-response behaviors at exposure levels below those at which SCC were seen experimentally. The overall model consisted of three linked modules. First, an anatomically realistic three-dimensional computational fluid dynamics (CFD) model described rat nasal airflow and site-specific flux of formaldehyde into the tissue in which the nasal SCC developed. Flux was the dose driver for two modes of action describing noncancer effects in the tissue: formation of DNA–protein cross-links (DPX) and cytolethality/regenerative cellular proliferation (CRCP). Finally, a two-stage clonal growth model linked the

[1] To whom correspondence should be addressed at the Center for Computational Systems Biology & Human Health Assessment, CIIT Centers for Health Research, 6 Davis Drive, Research Triangle Park, NC 27709. Fax: (919) 558-1300. E-mail: rconolly@ciit.org.

[2] Current address: U.S. EPA, ORD, NHEERL, Research Triangle Park, NC 27711

[3] Current address: Wyeth-Ayerst Research, Collegeville, PA 19426

modes of action with mutation accumulation and tumor formation.

Here, we describe development of a human version of this formaldehyde-exposure tumor-response model. Our overall objective was to maximize the use of relevant mechanistic information in predicting the potential human cancer response to inhaled formaldehyde. The only structural difference between the rat and human models is inclusion of the entire respiratory tract in the human model. The rat model is restricted to the nasal airways. Inclusion of the entire respiratory tract in the current model provides a capability for prediction of tumor risk associated with oronasal breathing, as occurs at higher exertion levels and which is of concern for occupational exposures to formaldehyde.

The human model uses human data for parameterization as fully as possible and draws on data from laboratory animals only when relevant human data are not available. Parameterization consisted of identification of baseline parameter values associated with control levels of tumor incidence and specification of how formaldehyde exposure changes the baseline values. Human versions of the CFD model and a linked typical path model for the lower respiratory tract were used for predictions of regional dosimetry (Kimbell *et al*., 2001a; Overton *et al*., 2001). A human DPX model (Conolly *et al*., 2000) based on scale-up from rat and rhesus monkey DPX models was used to predict regional formation of DPX driven by the CFD-predicted flux of formaldehyde into tissue. CRCP data from the rat were used ''as is,'' since neither guidance on scale-up nor equivalent human data were available (Conolly *et al*., 2002). Finally, baseline parameter values for the human clonal growth model were calibrated against human lung cancer incidence data (Peto *et al*., 1992; SEER, 2003).

The tumor dose-response predicted by the rat model was sensitive to the shape of the dose-response for CRCP, as was expected from a theoretical study (Lutz and Kopp-Schneider, 1999). A J-shaped dose-response for tumor incidence was predicted when the measured dose-response for CRCP was used, notwithstanding a concurrent low-dose-linear dose response for DPX and associated direct mutagenicity. A hockey-stick-shaped transformation of the CRCP data provided a monotonically increasing tumor dose response. These alternative descriptions of CRCP dose response are also used in the present report, and the corresponding predictions of tumor risk are provided.

Biologically motivated computational modeling minimizes risk assessment uncertainty by describing, as accurately as possible, the mechanisms responsible for the response of interest. This approach provides insight into the biological basis of the response seen experimentally and is the preferred basis for extrapolation of the dose response outside the range of the data (U.S EPA, 1996). While uncertainties worthy of additional experimental and theoretical work exist in the current model, risk-conservative choices, described below, were made during its development. These choices, combined with the advantages obtained from maximal use of mechanistic data, mean that the new tumor risk predictions are conservative, even though these risks are smaller than were predicted by previous assessments.

MODEL DEVELOPMENT

The overall exposure-tumor response model (Fig. 1) links the inhaled concentration of formaldehyde in humans with development of respiratory tract cancer. This model and the earlier rat version (Conolly *et al*., 2003) are identical in many respects. The current manuscript does not repeat detailed descriptions of model components found in Conolly *et al*. (2003). Instead, brief overviews are given for the components that are common to the rat and human models, and detailed descriptions are provided only for components unique to the human model. Readers interested in the methodological details of the current manuscript are strongly encouraged to first read Conolly *et al*. (2003).

Respiratory Tract Dosimetry of Formaldehyde

Site-specific flux. Kimbell *et al*. (1993, 2001b) showed that the flux of formaldehyde from inhaled air into tissue lining the nose of the F344 rat varies in a site-specific manner. The predicted pattern of deposition in rats correlates with tissue effects such as formaldehyde-induced squamous metaplasia (Kimbell *et al*., 1997a) and with inhibition of nasal mucociliary function (Kimbell *et al*., 1993). Prediction of site-specific dosimetry throughout the human respiratory tract was thus an important aspect of the model development process. To provide site-specific predictions of flux for the entire human respiratory tract, a three-dimensional CFD model for the human nose (Subramaniam *et al*., 1998) was linked to a one-dimensional typical path model of the lower respiratory tract (Overton *et al*., 2001).

Site-specific predictions of flux are used in the model as dose drivers for DPX formation and for CRCP in cells lining the respiratory tract (Fig. 1). Since the flux-DPX and flux-CRCP relationships are nonlinear (Conolly *et al*., 2003), a strategy for partitioning the nasal surface into areas of similar flux was needed. The CFD-typical path model was used to partition the surface of the respiratory tract into discrete regions and to provide specific flux predictions for each of these regions. For the nose, this partitioning was based on predicted flux, with the entire flux range for the nasal airway lining tissue being divided into 20 equal segments or ''flux bins'' (Kimbell *et al*., 2001a). This particular approach to defining flux bins means that a given bin could be physically discontinuous across the nasal epithelium. For the remainder of the respiratory tract, partitioning was based on anatomical structure rather than on predicted flux (Overton *et al*., 2001). A total of 25 flux bins was used to describe the lower respiratory tract, with the bins corresponding to the

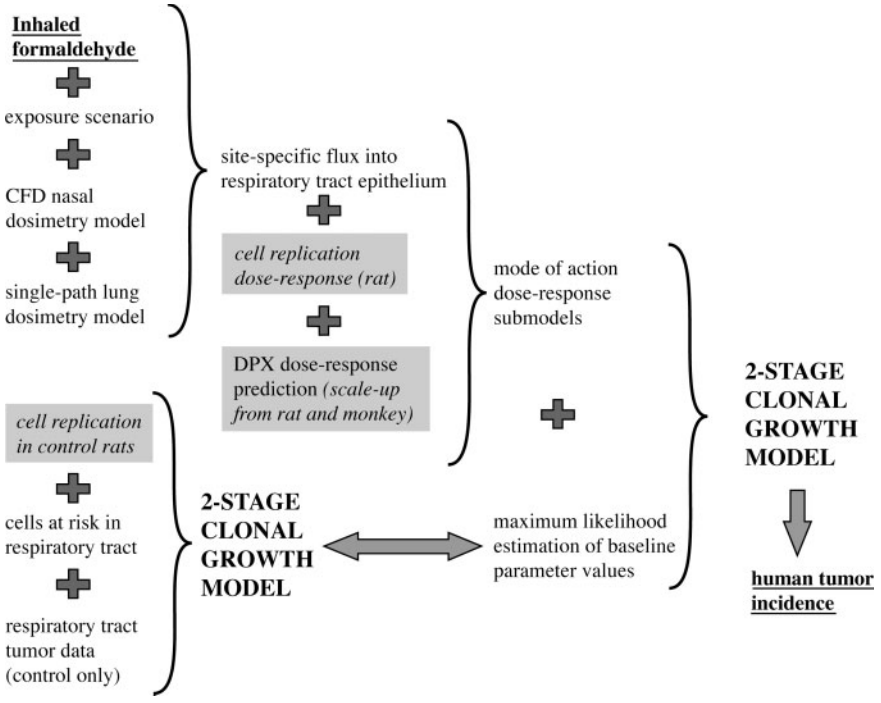

FIG. 1. Interrelationships of the major components of the human dose-response model for formaldehyde-induced respiratory tract cancer. Shaded boxes indicate data obtained in laboratory animals.

oral cavity and airway generations. The distally increasing surface area of the lower airways and the tendency of formaldehyde to move rapidly into the lining tissue results in the progressively more distal bins having less and less flux for a given inhaled concentration.

A sensitivity analysis was conducted on the number of nasal flux bins. This analysis consisted of predicting formaldehyde-associated human cancer risk while holding all parameters constant except for the number of flux bins. Risk predictions became stable (i.e., insensitive to the number of flux bins), between 10 and 15 bins (data not shown). We concluded that 20 flux bins were (more than) sufficient to describe the site-specific nature of the nasal dosimetry of formaldehyde.

Oronasal breathing and working levels. While the rat model described by Conolly *et al*. (2003) was restricted to the nasal airways, the current model encompasses the entire respiratory tract. Humans, unlike rats, are oronasal breathers, and oral breathing can introduce airborne formaldehyde directly into the upper airways of the lower respiratory tract. Casanova *et al*. (1991) showed that DPX are formed in proximal portions of the rhesus monkey lower respiratory tract, raising the possibility of a similar effect in humans. Some epidemiological studies (Blair *et al*., 1986, 1990; Gardner *et al*., 1993) reported an increase in lung cancer incidence associated with formaldehyde exposure, though others reported no such increases (Collins *et al*., 1997; Stayner *et al*., 1988). Concern thus exists for potential carcinogenic effects of formaldehyde throughout the human respiratory tract.

Since oronasal breathing typically occurs only at elevated exertion levels (also called working levels), formaldehyde dosimetry was predicted for several standard working levels promulgated by the International Commission on Radiological Protection (Table 1; Conolly *et al*., 2002; Snipes *et al*., 1997). These working levels describe the minute ventilation (i.e., ventilatory drive) for each hour of the day, and include combinations of nose-only and oronasal breathing. Working levels for a day spent not at work and for days of light and heavy working are described. Working level-specific risk prediction allowed examination of how changes in breathing rate and nose-only or oronasal breathing affect formaldehyde-related cancer risk.

TABLE 1
Working levels

Working level classification	Time (h) per day spent at activity level			
	Sleeping (7.5 l/min)[a]	Sitting (9.0 l/min)[a]	Light activity (25 l/min)[a]	Heavy activity (50 l/min)[a,b]
(1) Day not at work	8	8	8	—
(2) Light working	8	6	9	1
(3) Heavy working	8	4	10	2

[a]Minute ventilation.
[b]Heavy activity breathing rate is oronasal. All other breathing rates are nasal only.

Flux predictions. The CFD-typical path model was used to generate flux predictions for each flux bin for the various minute ventilation rates (7.5, 9.0, 25, and 50 l/min; Table 2)

TABLE 2
Flux Bins: Cells at Risk and Flux of Formaldehyde

Flux bin designation[a]	Number of cells at risk	Minute ventilation (l/m)			
		7.5	9	25	50
		Flux (pmol/mm^2/h/ppm)			
Nasal 1	2.3396E+07	9.9200E+01	1.3295E+02	8.4050E+02	7.2750E+02
Nasal 2	1.6547E+08	1.4755E+02	1.9935E+02	1.2505E+03	1.0775E+03
Nasal 3	8.4513E+07	2.5615E+02	3.3250E+02	1.5400E+03	1.3530E+03
Nasal 4	6.0153E+07	3.5905E+02	4.5055E+02	1.6510E+03	1.4750E+03
Nasal 5	4.6198E+07	4.6915E+02	5.7570E+02	1.7995E+03	1.6285E+03
Nasal 6	5.2097E+07	5.7235E+02	6.8340E+02	1.5970E+03	1.4940E+03
Nasal 7	4.7458E+07	6.7540E+02	7.8805E+02	1.6240E+03	1.5400E+03
Nasal 8	4.8778E+07	7.8085E+02	8.9260E+02	1.6415E+03	1.5745E+03
Nasal 9	4.6150E+07	8.8475E+02	9.8805E+02	1.6270E+03	1.5760E+03
Nasal 10	4.4383E+07	9.8900E+02	1.0860E+03	1.6375E+03	1.5975E+03
Nasal 11	4.1628E+07	1.0916E+03	1.1843E+03	1.6910E+03	1.6570E+03
Nasal 12	3.2933E+07	1.1958E+03	1.2806E+03	1.7285E+03	1.7005E+03
Nasal 13	2.8143E+07	1.3009E+03	1.3842E+03	1.8030E+03	1.7780E+03
Nasal 14	2.2527E+07	1.4018E+03	1.4786E+03	2.0055E+03	1.9535E+03
Nasal 15	1.3613E+07	1.5056E+03	1.5764E+03	2.0510E+03	2.0050E+03
Nasal 16	8.0801E+06	1.6050E+03	1.6819E+03	2.1645E+03	2.1180E+03
Nasal 17	2.9067E+06	1.7053E+03	1.7932E+03	2.1280E+03	2.1090E+03
Nasal 18	5.2933E+05	1.8134E+03	1.9051E+03	2.2820E+03	2.2600E+03
Nasal 19	1.6666E+05	1.9274E+03	2.0270E+03	2.5845E+03	2.5510E+03
Nasal 20	1.1814E+05	2.0378E+03	2.1465E+03	2.4560E+03	2.4340E+03
LRT 1	3.6681E+08	1.5179E+02	1.9567E+02	5.4752E+02	1.1328E+03
LRT 2	8.5277E+07	1.4421E+02	1.8970E+02	5.4346E+02	1.1683E+03
LRT 3	4.6116E+07	1.3641E+02	1.8235E+02	5.4602E+02	1.1908E+03
LRT 4	5.3574E+07	1.4214E+02	1.9132E+02	5.7803E+02	1.2564E+03
LRT 5	2.9662E+07	1.4728E+02	1.9899E+02	6.0233E+02	1.3047E+03
LRT 6	8.1747E+07	1.2704E+02	1.7409E+02	5.5470E+02	1.2320E+03
LRT 7	1.0367E+08	1.0955E+02	1.5370E+02	5.2813E+02	1.2019E+03
LRT 8	1.5889E+08	8.4824E+01	1.2325E+02	4.7699E+02	1.1294E+03
LRT 9	2.1562E+08	5.9032E+01	9.0190E+01	4.1553E+02	1.0407E+03
LRT 10	3.0086E+08	3.4968E+01	5.7289E+01	3.3943E+02	9.2284E+02
LRT 11	4.2117E+08	1.6941E+01	3.0497E+01	2.5685E+02	7.8599E+02
LRT 12	6.0247E+08	6.2252E+00	1.2684E+01	1.7266E+02	6.2596E+02
LRT 13	8.6579E+08	1.6023E+00	3.8238E+00	9.8386E+01	4.5216E+02
LRT 14	1.3572E+08	2.6018E−01	7.5560E−01	4.4236E+01	2.8118E+02
LRT 15	1.9549E+08	2.4956E−02	9.1601E−02	1.4893E+01	1.4493E+02
LRT 16	2.9284E+08	1.3261E−03	6.3242E−03	3.4457E+00	5.7651E+01
LRT 17	4.4422E+08	3.6306E−05	2.2844E−04	4.9356E−01	1.6161E+01
LRT 18	6.6744E+08	5.2142E−07	4.2912E−06	4.0153E−02	2.8946E+00
LRT 19	1.1198E+08	3.4839E−09	3.5332E−08	1.2566E−03	2.1571E−01
LRT 20	2.3154E+08	7.1130E−12	8.3729E−11	9.6440E−06	4.3740E−03
LRT 21	5.1461E+08	8.6665E−15	1.0987E−13	2.5890E−08	2.5314E−05
LRT 22	1.4643E+09	5.8642E−18	7.6454E−17	2.5235E−11	3.8502E−08
LRT 23	2.9029E+09	1.9368E−21	2.5364E−20	9.3979E−15	1.7203E−11
LRT 24	5.8315E+09	1.0164E−24	1.3259E−23	5.0160E−18	9.6200E−15
LRT 25	9.9161E+09	8.7659E−28	1.1360E−26	4.2367E−21	8.0693E−18

[a]Nasal: Nasal flux bins defined by the CFD model (Kimbell *et al.*, 2001)
LRT: Lower respiratory tract flux bins defined by the typical path model (Overton *et al.*, 2001)

associated with the working levels. For computation of DPX levels in each flux bin, the hour-by-hour changes in flux driven by the working levels were used as inputs to the DPX submodel (Conolly *et al*., 2000). For computation of the cell division rates, time-weighted average fluxes were calculated, as it did not seem reasonable to assume that the process of regenerative proliferation would vary on an hour-by-hour basis in direct proportion to the hour-by-hour variations in flux (Conolly *et al*., 2002, 2003). Time-weighted average fluxes were calculated for an exposure interval of one

TABLE 3
Formaldehyde Flux and Cell Division Rate Constants for Humans[a]

Flux[b] (pmol/mm^2/h)	Division rate constant (α) (1/hr)	
	Based on raw labeling index data	Based on hockey stick model for labeling index
0.00×10^0	4.19×10^{-4}	3.45×10^{-4}
4.36×10^2	3.20×10^{-4}	3.45×10^{-4}
1.24×10^3	2.97×10^{-4}	3.45×10^{-4}
3.74×10^3	6.04×10^{-4}	6.04×10^{-4}
6.23×10^3	2.09×10^{-3}	2.09×10^{-3}
9.34×10^3	4.24×10^{-3}	4.24×10^{-3}

[a]For methodological details see Model Development section of this manuscript and also Conolly *et al*. (2003).

[b]Fluxes predicted by the CFD model for the F344 rat nasal passages at sites where labeling index was measured.

week to capture hour-by-hour variations in flux during a day and also the effect of exposures for less than 7 days/week (i.e., typically 5 days/week with the weekend off). Having calculated time-weighted average flux, a corresponding single value for the rate of cell proliferation was calculated as described below (Table 3). In other words, a constant rate of cell division was associated with a particular formaldehyde exposure scenario. Time-weighted averaging was conducted as follows:

For working level classification 1 (Table 1), the time-weighted average flux in flux bin i is given by:

$$Flux_{i,1} = \frac{A_i + B_i + C_i}{3} \quad (1)$$

where A_i, B_i, and C_i are the predicted fluxes for the minute ventilation levels of 7.5, 9.0, and 25. l/min, respectively. Working level 1 describes a daily breathing pattern associated with a resting or very light activity level. For working level classifications 2 and 3, the calculations assume that 2 days a week are spent at working level 1 with the rest of the week spent at either working level 2 or 3, which correspond to higher levels of activity associated with physical labor or exercise, with level 3 being the most vigorous. For working level 2, the time-weighted average flux in bin i is given by:

$$Flux_{i,2} = \left(\frac{5}{7}\right) \cdot \frac{8 \cdot A_i + 6 \cdot B_i + 9 \cdot C_i + 1 \cdot D_i}{24} + \left(\frac{2}{7}\right) \cdot \frac{A_i + B_i + C_i}{3} \quad (2)$$

where A_i, B_i, C_i, and D_i are the bin-specific fluxes for the 7.5, 9.0, 25. and 50. l/min breathing rates, respectively. For working level 3, the time-weighted average flux in bin i is given by:

$$Flux_{i,3} = \left(\frac{5}{7}\right) \cdot \frac{8 \cdot A_i + 4 \cdot B_i + 10 \cdot C_i + 2 \cdot D_i}{24} + \left(\frac{2}{7}\right) \cdot \frac{A_i + B_i + C_i}{3} \quad (3)$$

Modes of Action Linking Regional Dosimetry with Tumor Response

DNA-protein cross-links. Formaldehyde is genotoxic and mutagenic (Heck *et al*., 1990), and formaldehyde inhalation leads to the formation of DPX in the nasal mucosa of rats (Casanova *et al*., 1994). DPX data have been used as a measure of tissue dose in cancer risk assessments for formaldehyde (Hernandez *et al*., 1994; Starr, 1990). Merk and Speit (1998) found, however, that DPX were not correlated with gene mutations in V79 cells at subcytotoxic doses. In the current model, DPX are nevertheless linked to the probability of procarcinogenic mutation per cell division. Since the role of DPX in mutation formation is in question, the description of a promutagenic role for DPX in the current model can be interpreted as a surrogate for the actual, but uncharacterized, directly mutagenic pathways of formaldehyde.

Dose-response and time-course data on DPX concentrations in the nasal mucosa of F344 rats were collected by Casanova *et al*. (1994). Casanova *et al*. (1991) measured DPX at several sites in the rhesus monkey nose exposed to various concentrations of formaldehyde. Both the rat and monkey data were used in development of a computational model of DPX formation (Conolly *et al*., 2000). This model uses flux into tissue as the input, describes saturable metabolic clearance of formaldehyde, a first-order clearance pathway to account for the innate reactivity of formaldehyde, and a pseudo-first-order reaction of formaldehyde with DNA to produce DPX. First-order clearance of DPX is also described, since Casanova *et al*. (1994) showed that DPX do not accumulate with repeated daily exposures. Quievryn and Zhitkovich (2000) found that DPX are removed from human cell lines by a combination of enzymatic repair and spontaneous hydrolysis.

The scaling behaviors of the DPX model parameters between rats and monkeys were calculated and used to predict parameter values for the human version of the DPX model, since no DPX data were available for humans (Conolly *et al*., 2000). The human DPX model is low-dose-linear for DPX formation (since DNA reactivity is first-order, and all clearance pathways in the model are effectively linear at low doses). At higher doses DPX are predicted to increase in a greater-than-linear manner due to saturation of the metabolic clearance of formaldehyde.

The human version of the DPX model could have been embedded within the larger risk model to calculate DPX values simultaneously with the calculation of tumor incidence. However, we calculated DPX values in advance and used tables of

these precomputed values as inputs to the clonal growth model. This approach avoided the need for numerical integration to compute DPX values while computing the other quantities of the overall model and provided a substantial increase in computational throughput.

Cytotoxicity-regenerative cellular proliferation. The reactivity of formaldehyde leads, at sufficiently high doses, to frank cytolethality followed by regenerative cellular proliferation. The present model describes an empirical linkage between flux into tissue and regenerative proliferation (Table 3). An explicit description of the killing of cells by formaldehyde and use of the resulting cell deficit to drive regenerative proliferation is not included in the present model. In linking flux directly to regenerative proliferation, we assumed that measured regenerative proliferation is a quantitatively accurate surrogate for the cytolethality of formaldehyde.

Conolly *et al*. (2003) describe in detail how the labeling index data obtained by Monticello *et al*. (1991, 1996) in the F344 rat were used to calculate division rate constants. Since no equivalent human labeling index data were available, we used the rat data in calculating the human division rate constants (Table 3). The details of the calculation for humans were identical to those for rats, except that the fraction of cells (*f*) at risk used for the human calculation was 0.668, while *f* for the rat was 0.819. The parameter *f* represents cells with replicative potential considered to be at risk of acquiring mutations that can lead to cancer. Cells that are terminally differentiated are thus considered to be not at risk. Given the variation among species in the cellular composition of various respiratory tract regions (Harkema *et al*., 1987; Mercer *et al*., 1994; Stone *et al*., 1992) one would expect the value for *f* to vary throughout the human respiratory tract. The value for *f* of 0.668 is appropriate for the human nasal mucosa where inhaled formaldehyde is predicted to exert most of its DNA-damaging and cytotoxic effects. The division rate constant (α) is obtained from the labeling index (*LI*), the duration of exposure to label (*t*) and *f* by:

$$\alpha = \frac{1}{2t} \cdot \ln\left(\frac{1}{1 - \frac{LI}{f}}\right) \quad \text{for } LI < f \tag{4}$$

Since *f* varies between rats and humans, the division rate constants used for the human model (Table 3) are slightly larger than the equivalent numbers used in the rat model (Conolly *et al*., 2003), even though the same labeling index data were used for the two calculations. To summarize, this approach to calculating the human division rate constants assumes that (1) the labeling indices arising from identical exposures to formaldehyde in rats and humans are the same and (2) the fractions of cells at risk (i.e., having replicative potential) are different.

One of the subtleties in calculating the dose response for division rate constants from the rat data arises from the fact that the rat CFD model predicts that the site of highest flux in the rat nose is not within the sites where labeling index was measured experimentally (Conolly *et al*., 2003). The largest labeling index measured experimentally is thus probably not the largest labeling index that actually occurs in response to cytolethal exposures to formaldehyde. The division rate constant corresponding to the largest predicted flux (designated α_{max}) was estimated by maximum likelihood (Table 4; Conolly *et al*., 2003). The value of α_{max} so obtained, 4.35×10^{-2}/h, corresponds to a cell cycle time of about 23 h and is similar to estimates of the cell cycle time that can be calculated from the literature. Evans and Shami (1989) reported that total times for transition through DNA synthesis, G2, and mitosis for respiratory tract basal cells and nonciliated columnar cells were 15.4 h (range 14.3–16.6 h) and 12.0 h (range 10.1–14.0 h), respectively. Hotchkiss *et al*. (1997) estimated that time for transition of these cell types through G0 is 12–20 h, with the lower end of this range appearing to be more realistic. These experimental data provide a range of complete cell cycle times for basal, nonciliated columnar and type II cells (i.e., progenitor cells) from 22 thorough about 36 h, with a preference for the lower end of the range. The range observed experimentally and the value obtained computationally are thus consistent with each other.

A second subtlety concerning the dose-response for the cell division rate constants comes from the shape of the dose-response curve for the labeling index. Monticello *et al*. (1991, 1996) measured the labeling index in the F344 rat nose after

TABLE 4
Parameter Values for the Human Clonal Growth Model

	J-shaped CRCP			Hockey stick CRCP		
Parameter	Nonsmoking	Mixed	Smoking	Nonsmoking	Mixed	Smoking
multb	1.015	1.017	1.020	1.024	1.020	1.024
multfc	2.583	2.583	2.583	2.515	2.515	2.515
μ_{Nbasal}	1.655E−09	5.709E−09	5.941E−09	1.267E−09	7.238E−09	7.627E−09
KMU	5.014E−10	1.729E−09	1.799E−09	3.525E−10	2.014E−09	2.122E−09
D	3.5 years	3.5 years	3.5 years	3.5 years	3.5 years	3.5 years
α_{max}[a]	0.0435	0.0435	0.0435	0.0435	0.0435	0.0435

Note. See Table 5 for parameter descriptions.
[a]Division rate constant associated with the maximum flux predicted by the CFD-single path dosimetry model.

exposure to 0, 0.7, 2, 6, 10, and 15 ppm formaldehyde. A J-shaped dose-response curve was obtained, with the means at 0.7 and 2 ppm below control and the means at 6, 10 and 15 ppm above control (Conolly *et al*., 2002, 2003). The 95% confidence intervals on means at 0.7 and 2 ppm, however, included the overall mean for the combined data from the 0, 0.7, and 2 ppm groups. The J-shape in the data was thus interpreted as being not significantly different from a threshold model with the threshold set above 2 ppm. Since the tumor risk predicted by clonal growth models is extremely sensitive to cell kinetics (Gaylor and Zheng, 1996; Lutz and Kopp-Schneider, 1999), we decided to evaluate human cancer risk associated with formaldehyde exposure using both the raw J-shaped dose-response and a hockey stick–shaped transformation (i.e., a threshold-shaped dose-response) of the rat data (Conolly *et al*., 2002, 2003). Two empirical functions corresponding to the raw data and its hockey stick transformation, respectively, were thereby obtained relating flux into tissue with division rate constants (Table 3). Linear interpolation was used to determine values of the division rate constant consistent with flux values not specifically listed in Table 3.

Clonal Growth Model

Model structure. The two-stage clonal growth model used for this analysis (Fig. 2) is identical in its biological structure to other two-stage models (also called MVK models) that have been described in recent years (Cohen and Ellwein, 1990; Moolgavkar and Knudsen, 1981; Moolgavkar and Venzon, 1979; Moolgavkar *et al*., 1988; Portier and Kopp-Schneider, 1991). The model describes two populations: one of normal cells and one of intermediate cells having one mutation. Mutations are specified as arising during the process of cell division, so that the mutation parameter (μ) is a probability; i.e., the probability of mutation per division (or, more correctly, per cell generation). For the model, it is assumed that a tumor cell arises when an intermediate cell acquires a second mutation. Clinically observable tumors are assumed to arise by clonal expansion of this single progenitor. The time needed for this clonal expansion is incorporated into the model through use of a delay function where a clinically observable tumor (detected either microscopically or grossly) was described as appearing at the end of a fixed interval from the birth of its progenitor cell. The sources of parameter values are described below and are summarized in Table 5.

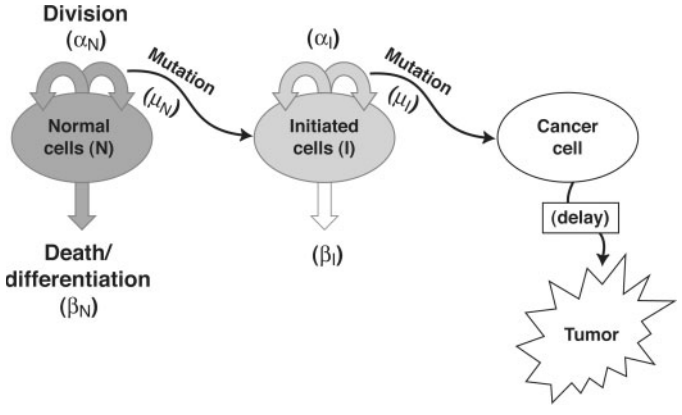

FIG. 2. Two-stage clonal growth model. The biological structure depicted is the same as that for the "MVK" model. α: division rate constant (1/h); β: death rate constant (1/h), μ: probability of mutation per cell division.

Equations. The model was written in the simulation language ACSL (The AEgis Technologies Group, Huntsville, AL). A discrete time implementation was used, with the analytical expression for growth of cell populations used across time steps (Δt) of 1 h. The Nelder-Mead algorithm as implemented in ACSL Math was used for likelihood maximization. A copy of the computer code is available from RBC (rconolly@ciit.org).

The total number of normal cells at risk (N) as a function of age in h (t) (i.e., the number of N cells in all the flux bins combined) was assumed to be proportional to body weight:

$$N(t) = N_{adult}\left(\frac{BW(t)}{BW_{adult}}\right) \tag{5}$$

N_{adult} is the total number of normal cells at risk in the adult, $BW(t)$ is body weight in kg at age t and BW_{adult} is adult body weight. A Gompertz curve was fitted to age-dependent body weight data for human males (Fig. 3; Burmaster and Crouch, 1997) and used to specify $BW(t)$.

The probabilities of mutation of normal and intermediate cells per cell generation in flux bin i ($\mu_{N,i}$, $\mu_{I,i}$, respectively) have baseline values independent of formaldehyde exposure ($\mu_{N,basal}$, $\mu_{I,basal}$, respectively) and formaldehyde-dependent components that are functions of DPX:

$$\mu_{N,i} = \mu_{N,basal} + KMU \cdot DPX_i \tag{6a}$$

$$\mu_{I,i} = \mu_{I,basal} + KMU \cdot DPX_i \tag{6b}$$

KMU (mm^3/pmol) is a proportionality constant, and DPX_i (pmol/mm^3) is the DNA–protein crosslink concentration in bin i. $\mu_{N,basal}$ and $\mu_{I,basal}$ are estimated by maximum likelihood. KMU was calculated using the approach described by Moolgavkar *et al*. (1999):

$$KMU = KMU_{rat}\left(\frac{\mu_{N,basal-human}}{\mu_{N,basal-rat}}\right) \tag{7}$$

where KMU_{rat} is the rat value for KMU (Conolly *et al*., 2003), and $\mu_{N,basal\text{-}human}$ and $\mu_{N,basal\text{-}rat}$ are the human and rat values of $\mu_{N,basal}$, respectively. This approach to the estimation of the human value for KMU specifies that human cells are inherently more difficult to mutate than rodent cells. Numerous laboratory experiments have shown that neoplastic transformation is much more difficult to achieve with human than with rodent cells (Holliday, 1996). While mutation and neoplastic transformation may not be identical, the difficulty of transforming human cells

TABLE 5
Parameters of the Clonal Growth Model

Parameter	Description and units	Source
N	Number of normal cells at risk	Harkema *et al.*, 1987; Stone *et al.*, 1992; Mercer *et al.*, 1994.
I	Number of intermediate cells (cells with one mutation)	Equation 9.
α_N	Division rate constant for N cells (1/h)	Calculated from rat labeling index data (Monticello *et al.*, 1996) using human fraction of cells at risk (Equation 4).
α_I	Division rate constant for I cells (1/h)	Set equal to α_N.
α_{max}	Division rate constant at site of maximum flux in the rat nose predicted by CFD model	Uses rat value estimated by maximum likelihood (Conolly *et al.*, 2003).
β_I	Death/terminal differentiation rate constant for initiated cells (1/h)	Set equal to α_I.
multb	Defines a growth advantage for I cells in the absence of formaldehyde exposure	Estimated by maximum likelihood using human tumor incidence data (Peto *et al.*, 1992; SEER, 2003).
multfc	Defines the effect of formaldehyde exposure on the growth advantage for I cells.	Uses value for the rat (Conolly *et al.*, 2003).
μ_N	Total probability of mutation per cell generation for N cells.	Sum of baseline probability and probability due to formaldehyde (Equation 6). Set equal to μ_N.
μ_I	Total probability of mutation per cell generation for I cells.	Estimated by maximum likelihood using human tumor incidence data (Peto *et al.*, 1992; SEER, 2003). Set equal to μ_{Nbasal}.
μ_{Nbasal}	Baseline probability of mutation per cell generation for N cells.	Equation 7.
μ_{Ibasal}	Baseline probability of mutation per cell generation for I cells.	Fixed at 3.5 years (Doll and Peto, 1978; Moolgavkar *et al.*, 1989).
KMU	Proportionality constant relating tissue concentration of DPX to μ_N and μ_I.	
D	Time delay required for a single cell with two mutations to expand clonally into a clinically detectable tumor.	

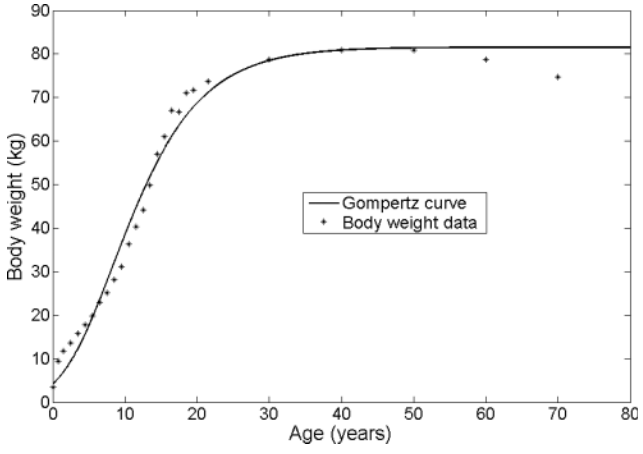

FIG. 3. Lifetime body weight data for human males from Burmaster and Crouch (1997) with fitted Gompertz curve. The decline in body weight indicated by the data for late in life cannot be predicted by the Gompetz equation.

does suggest that either, (1) human transformation requires more mutations than transformation of rodent cells or (2), it is more difficult to mutate human cells than rodent cells. Some combination of these two factors could also be operative. In any event, as long as the human model contains only two stages, either of these factors will result in smaller probabilities of mutation relative to rodent cells. Our approach to the definition of KMU_{human} is, therefore, consistent with the biological differences between rats and humans, even if the specific details of these differences are not fully understood.

The number of mutations of normal cells in flux bin *i* occurring during a time step Δt ($M_{N,(t-\Delta t,t),i}$) is a function of the number of cells at the start of the time step ($N(t)_i$), the division rate during the time step ($\alpha_{N,i}$), the length of the time step (Δt), and the probability of mutation per cell generation ($\mu_{N,i}$):

$$M_{N,(t-\Delta t,t),i} = \mu_{N,i}(t) \cdot N(t)_i (e^{\alpha_{N,i}(t) \cdot \Delta t} - 1) \quad (8)$$

This expression is a form of the classical analytical expression for an exponential growth process. The number of divisions during Δt is calculated and then multiplied by $\mu_{N,i}$ to get the number of mutations during Δt.

The change in the number of initiated (I) cells in bin *i* during a time step Δt is given by:

$$I_{(t-\Delta t,t),i} = I_i(t) e^{\Delta t(multf_i \cdot \alpha_{I,i}(t) - \beta_{I,i}(t))} + M_{N,(t-\Delta t,t),i} - C_i \quad (9)$$

where $\alpha_I(t)$ and $\beta_I(t)$ are the division and death rate constants (1/h) of initiated cells, $multf_i$ is a bin-specific factor that allows

formaldehyde to alter the growth rate of *I* cells (see below), and C_i is a stochastic correction that allows the overall model to describe the exact tumor incidence (Hoogenveen *et al*., 1999; Moolgavkar *et al*., 1988):

$$C_i = \Delta t \cdot multf_i \cdot \alpha_{I,i}(t) \cdot \mu_{I,i}(t) \cdot I_i(t)\left(1 + \frac{\Delta t \cdot I_i(t) \cdot multf_i \cdot \alpha_{I,i}(t)}{\sum_{t=0}^{t=T} M_{N,(t-\Delta t,t),i}}\right) \quad (10)$$

where *T* is the sum of the intervals Δt.

The flux bin-specific growth parameter for *I* cells, $multf_i$, consists of a baseline component (*multb*) that is independent of formaldehyde exposure and a formaldehyde-dependent component *multfc*:

$$multf_i = multb - multfc \cdot \max((\alpha_{I,flux_i} - \alpha_{I,basal}), 0) \quad (11)$$

The role of *multfc* is to decrease the growth advantage for *I* cells from the baseline value as flux increases. This decrease was found to be necessary when working with the rat tumor data (Conolly *et al*., 2003). The term $max((\alpha_{I,fluxi} - \alpha_{I,basal}), 0)$ is used, since negative values for $(\alpha_{I,flux_i} - \alpha_{I,basal})$ are possible with the J-shaped dose response for CRCP (Table 3). The rat value of *mutlfc* was used in the human model since its value was identified by maximizing the likelihood of the rat tumor data, and no information was available on how it should be scaled from rats to humans. It turns out, however, that *multfc* plays only a minimal role in predictions of human additional risk. With J-shaped CRCP up to about 1 ppm, inhaled formaldehyde decreases the division rate constant, and *multfc* does not affect the value of $multf_i$. With hockey-stick-shaped CRCP, fluxes of formaldehyde corresponding to the blade of the hockey stick (i.e., to its horizontal component) do not affect the value of $multf_i$. The lowest concentration at which *multfc* affects predictions of additional risk using hockey-stick-shaped CRCP is about 0.7 ppm. This predicted negative effect of formaldehyde on the growth advantage of *I* cells is much more important for describing the rat tumor does-response, where inhaled concentrations as high as 15 ppm were used.

The bin-specific mutation of initiated cells across a time step ($M_{I,(t-Dt,t)}$), is given by:

$$M_{I,(t-\Delta t,t),i} = \mu_{I,i}(t) \cdot I_i(t)(e^{multf_i \cdot \alpha_{I,i}(t) \cdot \Delta t} - 1) \quad (12)$$

The cumulative probability of tumor at age *T* is calculated by summing the mutation of intermediate cells across all the flux bins:

$$P(T) = 1 - e^{\left(-\sum_{i=1}^{binnum}\sum_{t=0}^{T} M_{I,(t-D-\Delta t,t-D),i}\right)} \quad (13)$$

where *D* is a delay representing the time required for a single cell created by mutation of a precursor initiated cell to expand clonally into a clinically detectable tumor, and *binnum* is the total number of flux bins.

Parameter estimation. Two parameters of the human model (*multb* and μ_N) were estimated by maximizing the Poisson log likelihood *LP*(*i*) of the 5-year age group incidence data (Tables 6 and 7):

$$LP(i) = \frac{e^{-u}u^i}{i!} \quad (14)$$

TABLE 6
Human Male Respiratory Tract Cancer Incidence, Age-Specific Crude Rates, Smokers and Nonsmokers Combined[a]

Age at diagnosis	Lung and bronchus	Oral cavity and pharynx	Larynx	Total
00–04	0.0	0.1	0.0	0.1
05–09	0.0	0.2	0.0	0.2
10–14	0.0	0.3	0.0	0.4
15–19	0.1	0.4	0.0	0.5
20–24	0.2	0.5	0.0	0.8
25–29	0.5	1.2	0.0	1.6
30–34	1.4	2.5	0.2	4.1
35–39	4.5	4.5	0.6	9.6
40–44	13.2	9.0	2.2	24.4
45–49	30.2	18.4	4.4	53.0
50–54	65.5	29.6	10.2	105.3
55–59	138.8	39.3	16.8	194.8
60–64	252.1	49.2	25.7	327.0
65–69	375.7	60.4	33.2	469.4
70–74	501.9	63.6	39.0	604.4
75–79	547.1	65.4	33.1	645.6
80–84	549.9	69.6	29.6	649.2
85+	462.6	68.0	24.3	554.9

[a]Annual incidence per 100,000 (SEER, 2003).

TABLE 7
Human Male Lung Respiratory Tract Cancer Mortality, Age-Specific Crude Rates, Smokers and Nonsmokers[a]

	Nonsmokers			Smokers		
Age at death	Lung cancer	Upper aero-digestive cancer[b]	Total incidence	Lung cancer	Upper aero-digestive cancer[b]	Total incidence
35–39	7	0	7	0	0	0
40–44	0	7	7	23	0	23
45–49	9	0	9	35	13	48
50–54	5	2	7	114	29	143
55–59	3	7	10	227	23	250
60–64	11	6	17	375	54	429
65–69	24	10	34	599	77	676
70–74	36	12	48	899	93	992
75–79	38	3	41	1,168	106	1,274
80+	88	10	98	1,191	154	1,345

[a]Annual incidence per 100,000 (Peto *et al*., 1992).
[b]Aero-digestive includes mouth, pharynx, larynx, and esophagus.

where $LP(i)$ is the probability of observing i events and u is the expected number of cases during the 5 year interval *Nyears*:

$$u = Nyears \cdot 10^5 \cdot \sum_{n=1}^{n=binnum} M_{I,(T-D-Nyears,T-D),n} \qquad (15)$$

Since the clonal growth model provides an incidence prediction for a single individual, the factor of 10^5 is used to adjust the model-generated prediction for comparison to the human data, which are provided as annual incidence/100,000.

Human Tumor Data

Development of the human risk model for formaldehyde requires identification of baseline parameter values (i.e., the values of parameters in the absence of exposure to formaldehyde). These parameter values were estimated by maximum likelihood using human tumor incidence data not explicitly related to formaldehyde exposure. Age-specific respiratory tract tumor incidence data are available from the U.S. National Cancer Institute's Surveillance, Epidemiology and End Results (SEER) database (SEER, 2003). SEER provides data for combined lung and bronchus, combined oral cavity and pharynx, and for larynx (Table 6). No data specifically for the nasal tissues or the nasopharynx are presented, which is presumably an indication of the comparative rarity of these tumors in the human population. SEER data for the tumors of primary concern based on the rodent bioassays, nasal squamous cell carcinoma, are thus not available.

The SEER database does not distinguish tumor incidence on the basis of smoking behavior. Estimates of lung cancer mortality in smoking and nonsmoking populations were available, however, from Peto *et al*. (1992; Table 7). Mortality data for lung cancer and for "upper aero-digestive cancer"—cancers of the mouth, pharynx, larynx or esophagus—are presented. Since the survival rate from lung cancer is low and the course of the disease is rapid, mortality is a reasonable surrogate for incidence of clinical detection of the cancer, as is provided by SEER (2003).

Baseline values of the clonal growth parameters are determinants of the predicted cancer risks associated with formaldehyde exposure. For example, the probability of mutation per cell generation (μ_N; Equation 6) has a baseline component and a component related to the concentration of DPX. The rate at which cells acquire mutations and thereby move to the next stage in the clonal growth model is a multiplicative function of several parameters including μ_N. The increase in mutations of normal cells ($M_{N,(t-\Delta t,t)i}$; Equation 8) due to an effect of formaldehyde on α_N is proportional to μ_N. The specific data sets to which the baseline model is calibrated are thus determinants of the final risk predictions. For this reason, we chose to combine the available incidence data for various regions of the respiratory tract (Tables 6 and 7) to approximate overall respiratory tract cancer incidence. Use of the overall incidence can be viewed as a conservative approach to risk assessment, since maximizing the value of μ_N maximizes the predicted additional risks associated with formaldehyde exposure.

Three baseline calibrations—for the general population using the SEER (2003) data and for smokers and nonsmokers using Peto *et al*. (1992)—were obtained by maximizing the likelihoods of the data. These calibrations allowed us to predict separate additional risks as a function of smoking status.

RESULTS

Baseline Calibration against Respiratory Tract Cancer Incidence Data

Separate maximum likelihoods of the human tumor data were calculated for J- and hockey-stick-shaped CRCP. Each likelihood was obtained by simultaneously varying six parameters (*multb* and μ_{Nbasal} for the nonsmoking, mixed, and smoking incidence data, respectively). The optimal parameters (Table 4) provided a reasonable but not exact description of the data (Fig. 4). The strong association of human respiratory tract cancer with cigarette smoking was reflected most clearly in the values of μ_{Nbasal}, which specifies the baseline probability of mutation per cell generation. A smoking-related trend in the value of *multb*, which specifies the growth advantage for *I* cells, was seen for J-shaped but not the hockey-stick-shaped CRCP.

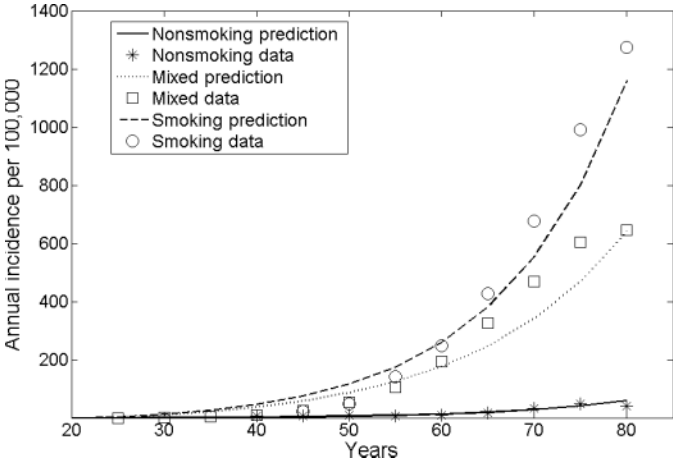

FIG. 4. Respiratory tract cancer incidence data for a mixed population of smokers and nonsmokers (SEER, 2003) and separately for nonsmokers and smokers (Peto *et al*., 1992). Optimal predictions of the data were obtained by maximizing the Poisson likelihood. This method was used to identify baseline values (i.e., values in the absence of exposure to formaldehyde) for parameters of the clonal growth model, as described in the Model Development Section. This prediction of the data was obtained using the control division rate constant for hockey-stick-shaped CRCP (Table 3). Use of the control division rate constant for J-shaped CRCP (Table 3) provided a visually identical fit to the data, though slightly different parameter estimates (Table 4).

Cancer Dose-Response Predictions

Cancer dose-response predictions were obtained for a total of 18 scenarios involving either continuous environmental exposure (Fig. 5; Table 8A), "light" (Table 8B), or "heavy" (Table 8C) working occupational scenarios. Each of these three categories included separate predictions for J- and hockey-stick-shaped CRCP. Within the J-shaped and hockey-stick-shaped subcategories, predictions were obtained for nonsmokers, a mixed population of nonsmokers and smokers, and for smokers.

By far the most dominant effect across all of the categories was exerted by the shape of the dose-response curve for CRCP (i.e., either J- or hockey-stick-shaped) (Table 3). All predicted risks associated with the J-shaped dose response for inhaled concentrations up to one ppm were predicted to be negative (Fig. 6; Table 8), meaning that these predicted additional risks were below the baseline (control) level. All predicted risks associated with the hockey-stick-shaped dose response for CRCP were positive. The low-dose linear component of these latter curves (e.g., Fig. 5) was due to the low-dose linear formation of DPX, which in the model produces a proportionate increase in the probability of mutation per cell generation. The upward inflection in predicted additional risk, using hockey-stick-shaped CRCP at about 0.7 ppm (e.g., Figs. 5 and 6) identifies the lowest concentration at which formaldehyde is predicted to change the rate of regenerative cellular proliferation

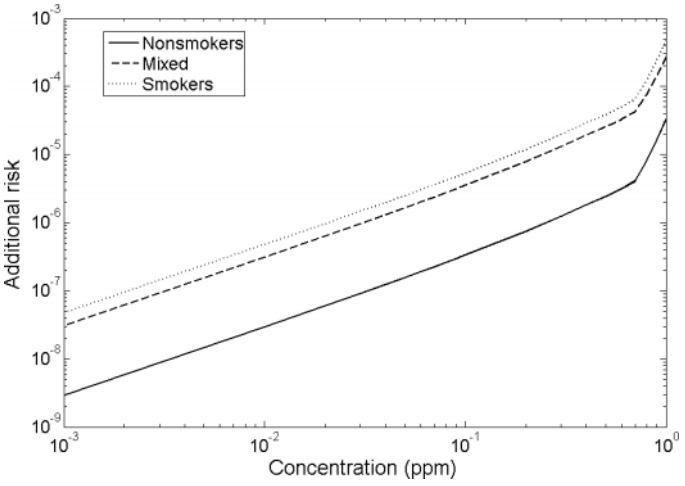

FIG. 5. Predicted additional risks for 80-year continuous environmental exposure to formaldehyde using hockey-stick-shaped CRCP. Predicted risks for smokers are about a factor of 10 greater than for nonsmokers. The curves are linear from 1 ppb (0.001 ppm), the lowest concentration evaluated, up to about 0.7 ppm, at which point the curve inflects upwards. The inflection occurs at the lowest inhaled concentration at which the model predicts effects of formaldehyde on the rate of regenerative cellular proliferation. The linear portions of the curves represent additional risk due solely to the effect, as described in the model, of DPX on the probability of mutation per cell division. This version of the tumor risk model is thus low dose linear, as the computational model for DPX formation (Conolly *et al*., 2000) is low dose linear.

TABLE 8
Cancer Dose-Response Predictions

	J-shaped CRCP			Hockey stick-shaped CRCP		
ppm	Nonsmoking	Mixed	Smoking	Nonsmoking	Mixed	Smoking
A. Predicted additional risks for continuous 80-year environmental exposure						
0.001	−1.04E−06	−9.78E−06	−1.69E−05	2.94E−09	3.11E−08	4.72E−08
0.010	−1.03E−05	−9.72E−05	−1.67E−04	2.97E−08	3.15E−07	4.77E−07
0.020	−2.05E−05	−1.93E−04	−3.32E−04	6.02E−08	6.37E−07	9.66E−07
0.030	−3.05E−05	−2.87E−04	−4.93E−04	9.14E−08	9.67E−07	1.47E−06
0.040	−4.04E−05	−3.80E−04	−6.52E−04	1.23E−07	1.31E−06	1.98E−06
0.050	−5.01E−05	−4.71E−04	−8.08E−04	1.56E−07	1.65E−06	2.51E−06
0.060	−5.97E−05	−5.61E−04	−9.61E−04	1.90E−07	2.01E−06	3.05E−06
0.070	−6.92E−05	−6.50E−04	−1.11E−03	2.24E−07	2.37E−06	3.60E−06
0.080	−7.85E−05	−7.37E−04	−1.26E−03	2.60E−07	2.75E−06	4.17E−06
0.090	−8.76E−05	−8.23E−04	−1.41E−03	2.96E−07	3.13E−06	4.75E−06
0.100	−9.67E−05	−9.08E−04	−1.55E−03	3.33E−07	3.52E−06	5.34E−06
0.200	−1.80E−04	−1.69E−03	−2.86E−03	7.50E−07	7.93E−06	1.20E−05
0.300	−2.52E−04	−2.37E−03	−3.96E−03	1.25E−06	1.32E−05	2.00E−05
0.400	−3.11E−04	−2.91E−03	−4.86E−03	1.81E−06	1.92E−05	2.91E−05
0.500	−3.58E−04	−3.36E−03	−5.58E−03	2.42E−06	2.56E−05	3.89E−05
0.600	−4.00E−04	−3.74E−03	−6.22E−03	3.09E−06	3.26E−05	4.95E−05
0.700	−4.37E−04	−4.09E−03	−6.78E−03	4.08E−06	4.24E−05	6.49E−05
0.800	−4.71E−04	−4.41E−03	−7.31E−03	7.94E−06	7.51E−05	1.21E−04
0.900	−5.00E−04	−4.69E−03	−7.75E−03	1.67E−05	1.45E−04	2.43E−04
1.000	−5.25E−04	−4.92E−03	−8.14E−03	3.29E−05	2.70E−04	4.65E−04

TABLE 8
Continued

	J-shaped CRCP			Hockey stick-shaped CRCP		
ppm	Nonsmoking	Mixed	Smoking	Nonsmoking	Mixed	Smoking
B. Predicted additional risks for "light work" occupational exposure						
0.010	−1.10E−05	−1.09E−04	−1.89E−04	1.46E−08	1.71E−07	2.56E−07
0.020	−2.02E−05	−2.03E−04	−3.51E−04	1.86E−08	2.36E−07	3.51E−07
0.030	−2.93E−05	−2.96E−04	−5.11E−04	2.27E−08	3.02E−07	4.48E−07
0.040	−3.83E−05	−3.88E−04	−6.69E−04	2.70E−08	3.70E−07	5.48E−07
0.050	−4.72E−05	−4.79E−04	−8.25E−04	3.13E−08	4.41E−07	6.51E−07
0.060	−5.61E−05	−5.68E−04	−9.78E−04	3.58E−08	5.13E−07	7.56E−07
0.070	−6.48E−05	−6.57E−04	−1.13E−03	4.03E−08	5.87E−07	8.64E−07
0.080	−7.34E−05	−7.44E−04	−1.28E−03	4.50E−08	6.63E−07	9.76E−07
0.090	−8.19E−05	−8.31E−04	−1.43E−03	4.98E−08	7.41E−07	1.09E−06
0.100	−9.03E−05	−9.16E−04	−1.57E−03	5.48E−08	8.21E−07	1.21E−06
0.200	−1.70E−04	−1.72E−03	−2.92E−03	1.11E−07	1.73E−06	2.54E−06
0.300	−2.39E−04	−2.40E−03	−4.06E−03	1.79E−07	2.83E−06	4.14E−06
0.400	−2.86E−04	−2.88E−03	−4.85E−03	2.55E−07	4.07E−06	5.95E−06
0.500	−3.26E−04	−3.28E−03	−5.52E−03	3.38E−07	5.41E−06	7.91E−06
0.600	−3.63E−04	−3.65E−03	−6.14E−03	4.56E−07	7.11E−06	1.05E−05
0.700	−3.98E−04	−4.00E−03	−6.71E−03	2.20E−06	2.36E−05	3.89E−05
0.800	−4.30E−04	−4.31E−03	−7.22E−03	7.19E−06	6.93E−05	1.19E−04
0.900	−4.54E−04	−4.56E−03	−7.63E−03	2.22E−05	2.05E−04	3.57E-04
1.000	−4.67E−04	−4.69E−03	−7.85E−03	4.92E−05	4.45E−04	7.85E-04
C. Predicted additional risks for "heavy work" occupational exposure						
0.010	−1.41E−05	−1.37E−04	−2.31E−04	1.06E−08	1.02E−07	1.52E−07
0.020	−2.64E−05	−2.58E−04	−4.36E−04	1.23E−08	1.28E−07	1.90E−07
0.030	−3.85E−05	−3.78E−04	−6.37E−04	1.40E−08	1.55E−07	2.27E−07
0.040	−5.04E−05	−4.96E−04	−8.36E−04	1.57E−08	1.82E−07	2.66E−07
0.050	−6.22E−05	−6.13E−04	−1.03E−03	1.75E−08	2.09E−07	3.05E−07
0.060	−7.39E−05	−7.29E−04	−1.22E−03	1.93E−08	2.37E−07	3.45E−07
0.070	−8.55E−05	−8.42E−04	−1.41E−03	2.11E−08	2.66E−07	3.85E−07
0.080	−9.69E−05	−9.55E−04	−1.60E−03	2.29E−08	2.94E−07	4.26E−07
0.090	−1.08E−04	−1.07E−03	−1.79E−03	2.48E−08	3.23E−07	4.67E−07
0.100	−1.19E−04	−1.18E−03	−1.97E−03	2.67E−08	3.53E−07	5.10E−07
0.200	−2.24E−04	−2.20E−03	−3.65E−03	4.74E−08	6.77E−07	9.72E−07
0.300	−3.09E−04	−3.02E−03	−4.98E−03	7.21E−08	1.06E−06	1.52E−06
0.400	−3.70E−04	−3.62E−03	−5.95E−03	1.02E−07	1.52E−06	2.17E−06
0.500	−4.25E−04	−4.16E−03	−6.82E−03	1.39E−07	2.09E−06	2.98E−06
0.600	−4.78E−04	−4.67E−03	−7.63E−03	3.70E−07	4.40E−06	6.73E−06
0.700	−5.24E−04	−5.11E−03	−8.34E−03	3.35E−06	3.08E−05	5.15E−05
0.800	−5.53E−04	−5.39E−03	−8.80E−03	1.88E−05	1.65E−04	2.81E−04
0.900	−5.66E−04	−5.51E−03	−9.00E−03	5.25E−05	4.56E−04	7.83E−04
1.000	−5.72E−04	−5.58E−03	−9.11E−03	9.24E−05	7.91E−04	1.37E−03

from its baseline value. The predicted dose responses using J-shaped CRCP also inflect upward in the vicinity of one ppm (Fig. 6) and eventually have positive additional risks at higher inhaled concentrations of formaldehyde.

The occupational exposure scenarios (Tables 8B and 8C) involved an 80-year lifetime with an environmental exposure level of four ppb (0.004 ppm). At age 18 years exposures for 8 hr/day, 5 days/wk were simulated for 40 years. For hockey-stick-shaped CRCP, from 10 ppb through 0.6 ppm, the predicted additional risks for light working were greater than the risks for heavy working. From 0.7 to one ppm predicted risks for heavy working exceeded those for light working. This unintuitive behavior is due to the greater amount of oronasal breathing associated with heavy working. The peak predicted nasal flux of formaldehyde at 25 l/min is larger than the peak flux predicted for 50 l/min (Table 2). This difference occurs because 25 l/min is a nose-only breathing rate, while 50 l/min is oronasal. The exposure of the nasal mucosa to inhaled formaldehyde thus decreases as we move from 25 l/min nose-only breathing to 50 l/min oronasal breathing. When the switch to oronasal

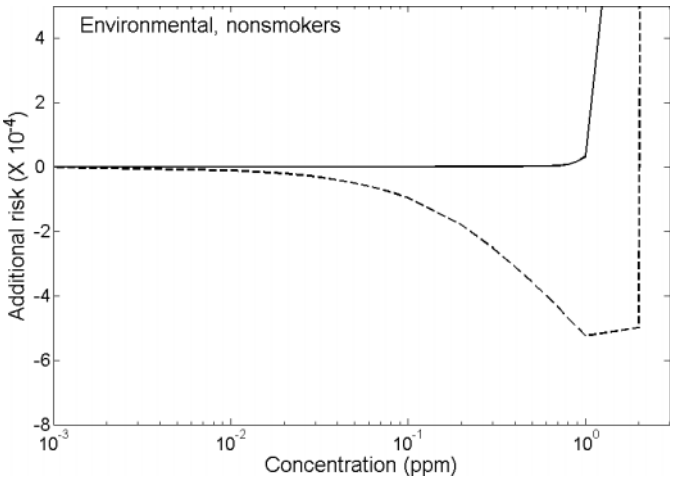

FIG. 6. Predicted additional risks for 80-year continuous environmental exposure to formaldehyde for nonsmokers. The negative values of additional risk, representing decreases cancer risk from its baseline (control) value, were predicted when J-shaped CRCP was used. Both curves inflect upwards when the flux of inhaled formaldehyde is sufficient to cause cytolethality and regenerative cellular proliferation. All dose-response predictions involving J-shaped CRCP showed qualitatively similar behaviors (Tables 8B and 8C). The dashed curve is angular at 1 and 2 ppm formaldehyde since no intermediate concentrations were evaluated. Note that in the current figure, additional risk is plotted on a linear scale, while in Figure 5 a log scale is used.

breathing occurs, cells in the upper segments of the LRT receive a considerably higher flux of formaldehyde from oral intake. From one ppb through 0.6 ppm, greater risk is predicted to occur by exposing fewer cells to higher flux. From 0.7 through one ppm, the greater risk is associated with exposure of larger numbers of cells. The switch between 0.6 and 0.7 ppm occurs because, at the higher inhaled concentrations, enough formaldehyde is predicted to be inhaled orally to result in stimulation of cell proliferation in the upper generations of the LRT. This predicted switchover behavior is another indication of the importance of formaldehyde-induced effects on regenerative proliferation.

DISCUSSION

Cancer is a disease characterized by loss of control of cell division (Cohen and Ellwein, 1990; Preston-Martin *et al*., 1990). Tumors arise when cells replicate without regard for the growth control signals that normally maintain a healthy balance between rates of division and apoptosis (Andersen *et al*., 1995). With the advent of multistage modeling of cancer, typical late-life cancers were first thought to be associated with six or more stages (Armitage and Doll, 1954). Armitage and Doll (1957), however, subsequently showed that two-stage models could accurately describe age-dependent incidence curves when cell replication within stages is considered. More recent work has suggested that, while some cancers, such as retinoblastoma, may in fact have two essential stages (Knudson, 2001; Moolgavkar and Knudson, 1981), others have more. Colorectal carcinoma, for example, appears to have four essential stages (Luebeck and Moolgavkar, 2002). Thus, the number of essential stages seems to vary with the specific kind of cancer. But both the literature on quantitative modeling of cancer incidence and the explosion of new information on the biology of cancer that has occurred in recent years clearly demonstrate a critical role for cell replication, regardless of the number of stages.

In maximizing the Poisson likelihood of the human tumor data (Tables 6 and 7), a tendency to overpredict incidence earlier in life and underpredict latter in life was seen (Fig. 4). Conolly *et al*. (2003) considered how changes in the number of stages in the model and in the value of the delay parameter (*D*; Tables 4 and 5) influence fits to time-to-tumor data. They also noted that the current two-stage model is probably not an accurate description of the actual mechanism of formaldehyde-induced cancer, and so some divergence of model predictions from the data is not surprising. It is likely that these same issues are also relevant to the quality of fit of the current model to the human respiratory tract cancers. Uncertainties about model structure and parameter values contribute to uncertainty in the final estimates of cancer risk. As described below, we have attempted to implement the model using conservative assumptions so that the risk predictions we present are conservative in the face of the modeling uncertainties.

The assessment described in this report was motivated to a large extent by our desire to incorporate as much relevant biology as possible. The formaldehyde database is characterized by an excellent dose-response dataset for CRCP in the F344 rat (Conolly *et al*., 2002; Monticello *et al*., 1991, 1996). Moolgavkar and co-workers (Luebeck and Moolgavkar, 2002; Moolgavkar and Knudson, 1981; Moolgavkar and Venzon, 1979; Moolgavkar *et al*., 1988, 1999), and others (Cohen and Ellwein, 1990; Portier and Kopp-Schneider, 1991) have shown how two-stage clonal growth models can be used to analyze cancer incidence data and provide insight into the relative roles of mutation and cell proliferation in the carcinogenic process. The approach we have taken for this new assessment of formaldehyde carcinogenicity thus stands on a body of work by investigators in risk assessment and cancer biology, working in academic, governmental, and private laboratories and dating back over twenty years.

Several cancer risk assessments for formaldehyde have been conducted since the first report of formaldehyde-induced nasal tumors in rats (Swenberg *et al*., 1980). When viewed in sequence, these assessments (Cohn, 1981; Hernandez *et al*., 1994; Schlosser *et al*., 2003; Starr, 1990; U.S. EPA, 1987) show increasing sophistication in the treatment of formaldehyde dosimetry and consistently lower predictions of risk when DPX are used as a measure of tissue dose in place of applied dose (inhaled ppm). With the exception of Schlosser *et al*. (2003), these assessments were conducted prior to the full publication of the dose-response data for CRCP obtained from the second

formaldehyde inhalation bioassay (Monticello *et al*., 1991, 1996). Schlosser *et al*. (2003) evaluated CRCP data in a benchmark dose-based assessment where the dose response for CRCP was used as a surrogate for the actual tumor response. No formaldehyde risk assessments published to date, however, have incorporated the dose response for CRCP into a clonal growth model. In addition to providing a biologically plausible framework for the inclusion of cell replication data, clonal growth modeling allows for evaluation of factors such as the multistage nature of the process and the time-dependent accumulation of preneoplastic lesions. These factors are associated with significant latent periods between carcinogen exposure and tumor development (Conolly *et al*., 2003; Lanphear and Buncher, 1992).

A further motivation for our approach was the availability of anatomically realistic nasal CFD models developed by Kimbell and coworkers (Kimbell *et al*., 1997a, 2001b; Subramaniam *et al*., 1998). These models describe how the complex anatomy of the nasal passages determines where inhaled formaldehyde contacts the tissue lining the airways. This capability was critical to a more realistic assessment, as the site-specific nature of both the acute lesions and the tumors that develop in response to formaldehyde exposure has been evident for some time (Kimbell *et al*., 1997b; Monticello *et al*., 1996; Morgan *et al*., 1986).

Conolly *et al*. (2003) describe how the clonal growth-based assessment of the cancer dose response for formaldehyde in the rat considered both relevant modes of action—direct mutagenicity and CRCP. The statistically optimal descriptions of the rat tumor data were associated with CRCP alone (i.e., with a complete lack of activity of the directly mutagenic pathway mediated by DPX). This result did not depend on the choice between J- and hockey-stick-shaped CRCP. Conolly *et al*. (2003) also found that use of the J-shaped CRCP provided a good fit to the tumor dose-response data while predicting a J-shaped dose-response at lower concentrations. This behavior occurred in spite of the concurrent activity of the DPX-mediated directly mutagenic pathway, indicating that the CRCP mode of action could dominate the directly mutagenic mode, in terms of their respective contributions to tumor incidence, as was shown in a theoretical study by Lutz and Kopp-Schneider (1999). Use of the hockey-stick-shaped cell replication led to a low-dose-linear dose response for additional risk reflecting the low-dose-linear activity of the DPX model of action in the dose range where formaldehyde is not affecting CRCP (i.e., in the blade of the hockey stock). The fit of the hockey stick model to the tumor data was identical to that of the J-shaped model.

As noted above, available data have not identified a direct correlation between DPX and mutation (Merk and Speit, 1998). The use of DPX in the current model is best viewed as a surrogate for any actual but unknown directly mutagenic action of inhaled formaldehyde. The high quality of the DPX data set and the good correlation between the nonlinearity in the dose response for DPX in the rat and that for formaldehyde-induced nasal SCC provide a level of comfort in this use of the DPX data. The conclusion that direct mutation does not play a significant role in the tumor response in the rat (and also in the human) should be robust for any potentially mutagenic effect of formaldehyde with a time course similar to that for DPX. The tissue time course for formaldehyde itself, for example, tracks closely with exposure, since free formaldehyde is rapidly cleared in the respiratory mucosa. This time course is similar to that for DPX, which do not accumulate in the rat with repeated daily exposure (Casanova *et al*., 1994) and are not expected to accumulate in humans (Conolly *et al*., 2000), though DPX are not predicted to be cleared as quickly as unbound formaldehyde. No dose-response data are available for other potentially mutagenic lesions associated with formaldehyde exposure. The options for describing a directly mutagenic mode of action for formaldehyde driven by something other than DPX are thus quite limited.

Motivated in part by the fact that the J-shaped dose-response reflected the raw data but also by the fact that at that time the J-shape was not thought to be statistically different from a hockey stick, Conolly *et al*. (2003, p. 432) stated that "...in light of modeling and database uncertainties, particularly the specification of the clonal growth model and the dose-response for CRCP, this work provides suggestive but not definitive evidence for a J-shaped dose-response curve for formaldehyde-mediated nasal SCC in the F344 rat." Since then, Gaylor *et al*. (2004) showed that the J-shape for CRCP is statistically significant for the posterior medial septum of the F344 rat nose. Other sites in the rat nose examined by Gaylor *et al*. (2004) did not show statistically significant J-shapes. This new statistical analysis and the theoretical study by Heck and Casanova (1999) increases, in our opinion, the likelihood that the low-dose dose response for formaldehyde-induced CRCP actually is J-shaped. We suspect that a statistically significant J-shaped dose response for CRCP would be detected if a new study were conducted with an optimal design.

Comparison of predicted risks from the current model with those of earlier assessments is not straightforward. The current model is based largely on maximum likelihood estimates (MLE) of its adjustable parameters and not on their upper bounds (though see the discussion below on use of an upper bound estimate for *KMU*). Upper bound estimates of extra risk ([total risk – baseline risk]/[1 – baseline risk]) were the focus of the earlier linearized multistage (LMS) and benchmark dose (BMD) assessments. As described by Schlosser *et al*. (2003), EPA (1987) used the LMS model to obtain a MLE risk estimate of 5.0×10^{-7} with an upper bound of 1.6×10^{-3} for continuous (70-year lifetime) exposure at 0.1 ppm. Use of DPX as a dosimeter rather than applied dose (inhaled ppm) tends to tighten the confidence interval around the MLE. While Schlosser *et al*. (2003) presented several alternative risk estimates obtained with BMD modeling, the MLE they reported for tumors of 1.3×10^{-3} with an upper bound of 1.4×10^{-3} for continuous (lifetime) exposure at 0.1 ppm is typical. (Neither the LMS nor the BMD approaches specified a length of exposure. However,

because they used tumor data from a two-year rat bioassay, the predicted risk is presumed to be associated with a standard human lifetime.)

Schlosser *et al*. (2003) used BMD software (Environ Corp., Ruston, LA) that allows for a nonzero ''threshold'' (the point at which the statistical function intercepts the x-axis). This approach provided the very tight error bounds around the MLE of risk described above. We believe this tight confidence limit is obtained because, due to the choice of statistical model and x-intercept variability, the benchmark point of departure ends up being close to the 6 ppm tumor incidence data-point, which has a good degree of statistical certainty.

The clonal growth model predicts 80-year lifetime additional risk (total risk minus baseline risk) of 3.3×10^{-7} for nonsmokers and 3.5×10^{-6} for a mixed smoking and nonsmoking population using hockey-stick-shaped CRCP data (Table 8). It should be noted that the clonal growth risk predictions at 0.1 ppm are driven by the value of *KMU*, the parameter that relates DPX to the probability of mutation per cell generation, since at 0.1 ppm, inhaled formaldehyde does not affect CRCP. Conolly *et al*. (2003) describe how a likelihood surface approach was used to derive an upper bound estimate for *KMU* in the rat, where the MLE estimate was 0. The human value of *KMU* used for our risk predictions, calculated using Equation 7, is thus risk conservative, since it is based on the rat upper bound for *KMU*. Use of the MLE estimate from the rat would have resulted in the human value of *KMU* also being 0 and would have led to a prediction of no (zero) additional lifetime risk at 0.1 ppm.

Although we have not developed a formal statistical analysis of confidence intervals around the risk predictions, we do think that the clonal growth model using hockey-stick-shaped CRCP is conservative in its predictions of risk. The main sources of this conservatism are: (1) prediction of additional risk using hockey-stick-shaped cell replication as opposed to the raw J-shape, (2) use of a nonzero value for *KMU*, the parameter linking DPX to the probability of mutation per cell division, when the optimal value of this parameter is 0, (3) prediction of risk for an 80-year lifetime rather than the EPA's default of 70 years, and (4) use of all the respiratory tract human incidence data (Peto *et al*., 1992; SEER, 2003) in developing the baseline calibration of the clonal growth model. Use of all the incidence data is conservative, because it maximizes the baseline values of the parameters. Formaldehyde-related additional risks are functions of the baseline parameter values. The larger these values, the larger the predicted additional risks. In addition to these conservative choices, several aspects of the new model are more realistic than previous models and can be expected to lead to more reliable assessments of risk. These more realistic aspects include (1) advanced dosimetry modeling, (2) partitioning of the respiratory tract surface area into 45 flux bins to capture the role of regional dosimetry on CRCP and DPX formation, and (3) a biologically motivated evaluation of how both CRCP and direct mutagenicity simultaneously affect tumor incidence.

A combination of formal sensitivity analysis and Monte Carlo-based analysis of model variability and uncertainty, as described by Allen *et al*. (1996), could be used to obtain upper bound estimates of risk from the clonal growth model. The version of the clonal growth model using the J-shaped dose-response for CRCP would be the appropriate starting point for such an analysis, since this is actual shape of measured dose-response curve.

The most striking feature of the predicted additional risks is the qualitative difference between predicted risks based on J- and hockey-stick-shaped CRCP (Table 8, Fig. 6). If the J-shaped predictions are accurate, then the respiratory tract carcinogenicity of formaldehyde is not a human health concern below about one ppm for any of the exposure scenarios evaluated (Table 8). If the hockey-stick-shaped dose-response is accurate, then for nonsmokers the predicted additional risk for 80 years of continuous environmental exposure is *de minimis* (10^{-6} or less) below 0.2 ppm, for the light working occupational scenario below 0.6 ppm, and for the heavy working scenario below 0.2 ppm. Given that these risk predictions are obtained from what are expected to be significant overestimates of real-world exposures to formaldehyde, we think that current exposure standards primarily concerned with noncancer effects of formaldehyde are sufficient for protection from potential carcinogenic effects. For example, the U.S. Occupational Safety and Health Administration Permissible Exposure Limit is 0.75 ppm as an 8-h time-weighted-average (OSHA, 2004), and the American Conference of Governmental Industrial Hygienists Limit is 0.3 ppm (ACGIH, 2004).

An earlier version of the current assessment (CIIT, 1999) has been used internationally in consideration of the cancer risks associated with formaldehyde exposure. The German MAK Commission concluded that the carcinogenic risks of formaldehyde are associated primarily with effects on cell proliferation (MAK, 2002). This interpretation means that exposure standards protective of effects on cell proliferation are expected to be protective against the potential carcinogenic effects of formaldehyde. Health Canada (2001) and the World Health Organization (WHO, 2002) used CIIT (1999) in their own assessments of formaldehyde. The Health Canada (2001) assessment of formaldehyde has been described in the peer-reviewed literature by Liteplo and Meek (2003).

An association of occupational exposure to formaldehyde with myeloid leukemia has recently been reported (Hauptmann *et al*., 2003). Heck and Casanova (2004) have addressed the biological plausibility of this distant site effect. They point out that formaldehyde inhalation does not result in measurable changes in blood levels of formaldehyde in rats or humans. The lack of an effect on blood levels is consistent with the innate reactivity of formaldehyde and with the expected steep concentration gradient from the airway surface into the mucosa (Schlosser *et al*., 2003). Our analysis indicates that, while the low dose, respiratory tract cancer risks from inhaled formaldehyde are either small or nonexistent, the dose-response curve at

one ppm and above is steep (Fig. 6). The predicted steepness is due to the nonlinear effects of formaldehyde on both CRCP and DPX in this concentration range. It would seem likely, therefore, that inhalation exposures above one ppm, as reported by Hauptmann *et al*. (2003) and sufficient to trigger a carcinogenic response in the bone marrow, would cause a larger carcinogenic response in the respiratory tract.

Our analysis of the respiratory tract cancer risks associated with formaldehyde exposure has emphasized quantitative, mechanistic factors such as CRCP and DPX and their respective dose-response behaviors. Heck and Casanova (2004) have emphasized, among other things, the importance of pharmacokinetic factors that determine tissue doses. While the association of occupational exposure to formaldehyde is interesting, it is important to recall the distinction between association and causation and to be prudent about suggesting causation when the database on pharmacokinetic and mechanistic factors suggests otherwise. As Hauptmann *et al*. (2003) noted in their findings, results for myeloid leukemia from other epidemiological investigations are mixed, suggesting a need for caution in drawing definitive conclusions from their study.

ACKNOWLEDGMENTS

Thanks to Dr. John Overton for his help with the dosimetry modeling and his thoughtful comments, to Drs. Suresh Moolgavkar and Georg Luebeck for their help with maximum likelihood calculations, and to Ms. Betsy Gross for her competent and cheerful assistance with data retrieval. We would also like to acknowledge the team of investigators at the Chemical Industry Institute of Toxicology (now the CIIT Centers for Health Research) who over the years provided much of the data without which this analysis would not have been possible. This team includes Drs. Jim Swenberg, Kevin Morgan, Henry Heck, and Tom Monticello, Ms. Mercedes Casanova and all the others who played critical roles in the development of these data.

REFERENCES

Allen, B. C., Covington, T. R., and Clewell, H. J. (1996). Investigation of the impact of pharmacokinetic variability and uncertainty on risks predicted with a pharmacokinetic model for chloroform. *Toxicology* **111,** 289–303.

American Conference of Governmental Industrial Hygienists (ACGIH). (2004). TLVs and BEIs. ACGIH, Cincinnati, OH. ISBN: 1-882417-54-2.

Andersen, M. E., Mills, J. J., Jirtle, R. L., and Greenlee, W. F. (1995). Negative selection in hepatic tumor promotion in relation to cancer risk assessment. *Toxicology* **102,** 223–237.

Armitage, P., and Doll, R. (1954). The age distribution of cancer and multi-stage theory of carcinogenesis. *Br. J. Cancer* **8,** 1–12.

Armitage, P., and Doll, R. (1957). A two-stage theory of carcinogenesis in relation to the age distribution of human cancer. *Br. J. Cancer* **11,** 161–169.

Blair, A., Stewart, P. A., and Hoover, R. N. (1990). Mortality from lung cancer among workers employed in formaldehyde industries. *Am. J. Ind. Med.* **17,** 683–699 (cited in IARC, 1995).

Blair, A., Stewart, P. A., O'Berg, M., Gaffey, W., Walrath, J., Ward, J., Bales, R., Kaplan, S., and Cubit, D. (1986). Mortality among industrial workers exposed to formaldehyde. *J. Natl. Cancer. Inst.* **76,** 1071–1084 (cited in IARC, 1995).

Burmaster, D. E., and Crouch, E. A. (1997). Lognormal distributions for body weight as a function of age for males and females in the United States, 1976–1980. *Risk Anal.* **17,** 499–505.

Casanova, M., Morgan, K. T., Gross, E. A., Moss, O. R., Heck, and Heck, d'A. (1994). DNA-protein cross-links and cell replication at specific sites in the nose of F344 rats exposed subchronically to formaldehyde. *Fundam. Appl. Toxicol.* **23,** 525–536.

Casanova, M., Morgan, K. T., Steinhagen, W. H., Everitt, J. I., Popp, J. A., and Heck, H. d'A. (1991). Covalent binding of inhaled formaldehyde to DNA in the respiratory tract of rhesus monkeys: Pharmacokinetics, rat-to-monkey interspecies scaling, and extrapolation to man. *Fundam. Appl. Toxicol.* **17,** 409–428.

Chemical Industry Institute of Toxicology (CIIT). (1999). *Formaldehyde: Hazard characterization and dose-response assessment for carcinogenicity by the route of inhalation,* revised ed. Chemical Industry Institute of Toxicology, Research Triangle Park, NC.

Cohen, S. M., and Ellwein, L. B. (1990). Cell proliferation in carcinogenesis. *Science* **249,** 1007–1011.

Cohn, M. S. (1981). Revised carcinogenic risk assessment of urea-formaldehyde foam insulation: Estimates of cancer risk due to inhalation of formaldehyde released by UFFI. U.S. Consumer Product Safety Commission, Washington, D.C.

Collins, J. J., Acquavella, J. F., and Esmen, N. A. (1997). An updated meta-analysis of formaldehyde exposure and upper respiratory cancers. *J. Occup. Environ. Med.* **39,** 639–651.

Conolly, R. B., Kimbell, J. S., Janszen, D. B., and Miller, F. J. (2002). Dose response for formaldehyde-induced cytotoxicity in the human respiratory tract. *Regul. Toxicol. Pharmacol.* **35,** 32–43.

Conolly, R. B., Kimbell, J. S., Janszen, D., Schlosser, P. M., Kalisak, D., Preston, J., and Miller, F. J. (2003). Biologically motivated computational modeling of formaldehyde carcinogenicity in the F344 rat. *Toxicol. Sci.* **75,** 432–447.

Conolly, R. B., Lilly, P. D., and Kimbell, J. S. (2000). Simulation modeling of the tissue disposition of formaldehyde to predict nasal DNA-protein cross-links in F344 rats, Rhesus monkeys, and humans. *Environ. Health Prespect.* **108** (Suppl. 5), 919–924.

Doll, R. and Peto, R. (1978). Cigarette smoking and bronchial carcinoma: Dose and time relationships among regular smokers and lifelong nonsmokers. *J. Epidemiol. Community Health* **32,** 303–313.

Evans, M. J., and Shami, S. G. (1989). Lung cell kinetics. In *Lung Cell Biology* (D. Massaro, Ed.), pp. 1–36, Marcel Dekker, New York.

Gardner, M. J., Pannett, B., Winter, P. D., and Cruddas, A. M. (1993). A cohort study of workers exposed to formaldehyde in the British chemical industry: An update. *Br. J. Ind. Med.* **50,** 827–834 (cited in IARC, 1995).

Gaylor, D. W., and Zheng, Q. (1996). Risk assessment of nongenotoxic carcinogens based upon cell proliferation/death rates in rodents. *Risk Anal.* **16,** 221–225.

Gaylor, D. W., Lutz, W.K., and Conolly, R. B. (2004). Statistical analysis of nonmonotonic dose-response relationships: Research design and analysis of nasal cell proliferation in rats exposed to formaldehyde. *Toxicol. Sci.* **77,** 158–164.

Harkema, J. R., Plopper, C. G., Hyde, D. M., Wilson, D. W., St. George, J. A., and Wong, V. J. (1987). Nonolfactory surface epithelium of the nasal cavity of the bonnet monkey: A morphologic and morphometric study of the transitional and respiratory epithelium. *Am. J. Anat.* **180,** 266–279.

Hauptmann, M., Lubin, J. H., Stewart, P. A., Hayes, R. B., and Blair, A. (2003). Mortality from lymphohematopoietic malignancies among workers in formaldehyde industries. *J. Natl. Cancer Inst.* **95,** 1615–1623.

Health Canada. (2001). Priority substances list assessment report: Formaldehyde. ISBN 0–662–29447–5. Cat. no. En40-215/61E.

Heck, H., and Casanova, M. (1999). Pharmacodynamics of formaldehyde: Applications of a model for the arrest of DNA replication by DNA-protein cross-links. *Toxicol. Appl. Pharmacol.* **160,** 86–100.

Heck, H. d'A., and Casanova, M. (2004). The implausibility of leukemia induction by formaldehyde: A critical review of the biological evidence on distant-site toxicity. *Regul. Toxicol. Pharmacol.* (accepted for publication).

Heck, H. D., Casanova, M., and Starr, T. B. (1990). Formaldehyde toxicity—new understanding. *Crit. Rev. Toxicol.* **20,** 397–426.

Hernandez, O., Rhomberg, L., Hogan, K., Siegel-Scott, C., Lai, D., Grindstaff, G. Henry, M., and Cotruvo, J. A. (1994). Risk assessment of formaldehyde. *J. Hazard. Mater.* **39,** 161–172.

Holliday, R. (1996). Neoplastic transformation: The contrasting stability of human and mouse cells. *Cancer Surv.* **28,** 103–115.

Hoogenveen, R. T., Clewell, H. J., Andersen, M. E., and Slob, W. (1999). An alternative exact solution of the two-stage clonal growth model of cancer. *Risk Anal.* **19,** 9–14.

Hotchkiss, J. A., Harkema, J. R., and Johnson, N. F. (1997). Kinetics of nasal epithelial cell loss and proliferation in F344 rats following a single exposure to 0.5 ppm ozone. *Toxicol. Appl. Pharmacol.* **143,** 75–82.

International Agency for Research on Cancer (IARC). (1995). Formaldehyde. In *Formaldehyde IARC Monographs on the Evaluation of Carcinogenic Risks to Humans*, Vol. 62, pp. 217–362, IARC, Lyon, France.

Kerns, W. D., Pavkov, K. L., Donofrio, D. J., Gralla, E. J., and Swenberg, J. A. (1983). Carcinogenicity of formaldehyde in rats and mice after long-term inhalation exposure. *Cancer Res.* **43,** 4382–4392.

Kimbell, J. S., Godo, M. N., Gross, E. A., Joyner, D. R., Richardson, R. B., and Morgan, K. T. (1997a). Computer simulation of inspiratory airflow in all regions of the F344 rat nasal passages. *Toxicol. Appl. Pharmacol.* **145,** 388–398.

Kimbell, J. S., Gross, E. A., Joyner, D. R., Godo, M. N., and Morgan, K. T. (1993). Application of computational fluid dynamics to regional dosimetry of inhaled chemicals in the upper respiratory tract of the rat. *Toxicol. Appl. Pharmacol.* **121,** 253–263.

Kimbell, J. S., Gross, E. A., Richardson, R. B., Conolly, R. B., and Morgan, K. T. (1997b). Correlation of regional formaldehyde flux predictions with the distribution of formaldehyde-induced squamous metaplasia in F344 rat nasal passages. *Mutat. Res.* **380,** 143–154.

Kimbell, J. S., Overton, J. H., Subramaniam, R. P., Schlosser, P. M., Morgan, K. T., Conolly, R. B., and Miller, F. J. (2001a). Dosimetry modeling of inhaled formaldehyde: Binning nasal flux predictions for quantitative risk assessment. *Toxicol Sci.* **64,** 111–121.

Kimbell, J. S., Subramaniam, R. P., Gross, E. A., Schlosser, P. M., and Morgan, K.T. (2001b). Dosimetry modeling of inhaled formaldehyde: Comparisons of local flux predictions in the rat, monkey, and human nasal passages. *Toxicol. Sci.* **64,** 100–110.

Knudson, A. G. (2001). Two genetic hits (more or less) to cancer. *Nat. Rev. Cancer* **1,** 157–162.

Lanphear, B. P., and Buncher, C. R. (1992). Latent period for malignant mesothelioma of occupational origin. *J. Occup. Med.* **34,** 718–721.

Liteplo, R. G., and Meek, M. E. (2003). Inhaled formaldehyde: Exposure estimation, hazard characterization, and exposure-response analysis. *J. Toxicol. Environ. Health. Part B,* **6,** 85–114.

Luebeck, E. G., and Moolgavkar, S. H. (2002). Multistage carcinogenesis and the incidence of colorectal cancer. *Proc. Natl. Acad. Sci. U.S.A.* **99,** 15095–15100.

Lutz, W. K., and Kopp-Schneider, A. (1999). Threshold dose response for tumor induction by genotoxic carcinogens modeled via cell-cycle delay. *Toxicol. Sci.* **49,** 110–115.

MAK Commission (2002). Formaldehyde, Official English Translation, Occupational Toxicants: Critical data evaluation for MAK values and classification of carcinogens, DFG, Deutsche Forschungsgemeinschaft, Commission for the Investigation of Health Hazards of Chemical Compounds in the Work Area, Vol. 17, 163–201, Wiley-VCH Weinheim (FRG).

Merk, O, and Speit, G. (1998). Significance of formaldehyde-induced DNA-protein crosslinks for mutagenesis. *Environ. Mol. Mutagen.* **32,** 260–268.

Mercer, R. R., Russell, M. L., Roggli, V. L., and Crapo, J. D. (1994). Cell number and distribution in human and rat airways. *Am. J. Respir. Cell Mol. Biol.* **10,** 613–624.

Monticello, T. M., Miller, F. J., and Morgan, K.T. (1991). Regional increases in rat nasal epithelial cell proliferation following acute and subchronic inhalation of formaldehyde. *Toxicol. Appl. Pharmacol.* **111,** 409–421.

Monticello, T. M., Swenberg, J. A., Gross, E. A., Leininger, J. R., Kimbell, J. S. Seilkop, S., Starr, T. B., Gibson, J. E., and Morgan K. T. (1996). Correlation of regional and nonlinear formaldehyde-induced nasal cancer with proliferating populations of cells. *Cancer Res.* **56,** 1012–1022.

Moolgavkar, S. H., and Venzon, D. J. (1979). Two-event models for carcinogenesis: Incidence curves for childhood and adult tumors. *Math. Biosci.* **47,** 55–77.

Moolgavkar, S. H., and Knudson, A. G. Jr. (1981). Mutation and cancer: A model for human carcinogenesis. *J. Nat. Cancer Inst.* **66,** 1037–1052.

Moolgavkar, S. H., Dewanji, A., and Venzon, D. J. (1988). A stochastic two-stage model for cancer risk assessment. I. The hazard function and the probability of tumor. *Risk Anal.* **8,** 383–392.

Moolgavkar, S. H., Dewanji, A., and Luebeck, G. (1989). Cigarette smoking and lung cancer: Reanalysis of the British doctors' data. *J. Natl. Cancer Inst.* **81,** 415–420.

Moolgavkar, S. H., Luebeck, E. G., Turim, J., and Hanna, L. (1999). Quantitative assessment of the risk of lung cancer associated with occupational exposure to refractory ceramic fibers. *Risk Anal.* **19,** 599–611.

Morgan, K. T., Jiang, X. Z., Starr, T. B., and Kerns, W. D. (1986). More precise localization of nasal tumors associated with chronic exposure of F-344 rats to formaldehyde gas. *Toxicol. Appl. Pharmacol.* **82,** 264–271.

Overton, J. H., Kimbell, J. S., and Miller, F. J. (2001). Dosimetry modeling of inhaled formaldehyde: The human respiratory tract. *Toxicol. Sci.* **64,** 122–134.

Peto, R., Lopez, A. D., Boreham, J., Thun, M., and Heath, C. (1992). Mortality from tobacco in developed countries: Indirect estimation from national vital statistics. *Lancet* **339,** 1268–1278.

Portier., C. J., and Kopp-Schneider, A. (1991). A multistage model of carcinogenesis incorporating DNA damage and repair. *Risk Anal.* **11,** 535–543.

Preston-Martin, S., Pike, M. C., Ross, R. K., Jones, P. A., and Henderson, B. E. (1990). Increased cell division as a cause of human cancer. *Cancer Res.* **50,** 7415–7421.

Quievryn, G., and Zhitkovich, A. (2000). Loss of DNA-protein crosslinks from formaldehyde-exposed cells occurs through spontaneous hydrolysis and an active repair process linked to proteosome function. *Carcinogenesis* **21,** 1573–1580.

Schlosser, P. M., Lilly, P. D., Conolly, R. B., Janszen, D. B., and Kimbell, J. S. (2003). Benchmark dose risk assessment for formaldehyde using airflow modeling and a single-compartment, DNA-protein cross-link dosimetry model to estimate human equivalent doses. *Risk Anal.* **23,** 473–487.

Surveillance, Epidemiology, and End Results (SEER) Program (www.seer.cancer.gov). (2003). SEER*Stat Database: Incidence—SEER 9 Regs Public-Use, Nov 2002 Sub (1973–2000), National Cancer Institute, DCCPS, Surveillance Research Program, Cancer Statistics Branch, released April 2003, based on the November 2002 submission.

Snipes, M. B.; James, A. C. and Jarabek, A. M. (1997). The 1994 ICRP66 human respiratory tract dosimetry model as a tool for predicting lung burdens from exposures to environmental aerosols. *Appl. Occup. Environ. Hyg.* **12,** 547–554.

Starr, T. B. (1990). Quantitative cancer risk estimation for formaldehyde. *Risk Anal.* **10,** 85–91.

Stayner, L. T., Elliott, L., Blade, L., Keenlyside, R., and Halperin, W. (1988). A retrospective cohort mortality study of workers exposed to formaldehyde in the garment industry. *Am. J. Ind. Med.* **13,** 667–681.

Stone, K. C., Mercer, R. R., Gehr, P., Stockstill, B., and Crapo, J. D. (1992). Allometric relationships of cell numbers and size in the mammalian lung. *Am. J. Respir. Cell Mol. Biol.* **6,** 235–243.

Subramaniam, R. P., Richardson, R. B., Morgan, K. T., Guilmette, R. A., and Kimbell, J. S. (1998). Computational fluid dynamics simulations of inspiratory airflow in the human nose and nasopharynx. *Inhal. Toxicol.* **10,** 92–120.

Swenberg, J. A., Kerns, W. D., Mitchell, R. I., Gralla, E. J., and Pavkov, K. L. (1980). Induction of squamous cell carcinomas of the rat nasal cavity by inhalation exposure to formaldehyde vapor. *Cancer Res.* **40,** 3398–3402.

U.S. Department of Labor, Occupational Safety and Health Administration (OSHA). (2004). Regulations (Standards—29 CFR) Formaldehyde.—1910.1048. Web address: (http://www.osha.gov/pls/oshaweb/owadisp.show_document?p_table=STANDARDS&p_id=10075), accessed May 17, 2004.

U.S. Environmental Protection Agency (U.S. EPA). (1987). Assessment of Health Risks to Garment Workers and Certain Home Residents from Exposure to Formaldehyde. Office of Pesticides and Toxic Substances, U.S. Environmental Protection Agency.

U.S. Environmental Protection Agency (U.S. EPA). (1996). Proposed guidelines for carcinogen risk assessment. Office of Research and Development, Washington, DC, EPA/600/P-92/003C, April 1996.

World Health Organization (WHO). (2002). Concise International Chemical Assessment Document 40: Formaldehyde. Geneva.